ARKIV FÖR FYSIK Band 16 nr 6

Communicated 11 March 1959 by Erik Hulthén and Erik Rudberg

Diffraction patterns of small phase objects measured in the microwave region

By Olof Bryngdahl

With 19 figures and 19 records in the text

ABSTRACT

Measurements were made on the diffraction patterns of circular phase objects by means of microwaves of 5.15-cm wavelength. The intensity of radiation in the electric plane was measured along the axis and close behind the diffracting object in several planes transverse to the incident beam direction. The patterns are compared with theoretical computations obtained using a modification of the Huygens-Kirchhoff theory of diffraction. Satisfactory agreement between experimental and theoretical curves was obtained.

1. Introduction

The development within recent years of measuring techniques for the electromagnetic centimeter waves has enabled the investigation of many optical phenomena which hitherto were beyond the reach of experimental methods. Recent measurements at microwave frequencies [1, 2, 3, 4, 5] have demonstrated the possibility of using the classical theory (i.e. Kirchhoff and its electromagnetic extensions) for diffraction experiments. Even though this theory is only an approximation, it gives an acceptable picture of the near field pattern.

The interpretation of the microscope out-of-focus effect on small non-absorbing phase objects gave the initial impulse to this examination [6, 7]. Objects of the size of a few wavelengths give rise to Fresnel diffraction effects in the near zone and, because of this, the appearance of the image changes upon defocusing, a phenomenon for which one has long desired a quantitative treatment. By means of microwaves, the field can be investigated, contrary to the situation in light optics, even in the immediate neighbourhood of a diffracting object, the dimensions of which can be of the order of magnitude of the wavelength. Hence, the present situation is such that the microwave region is in many respects more suited for the study of physical optics than the optical region itself. The results of such measurements go beyond the domain which can be investigated by optics and are, apart from the purely scientific interest they offer, also of great practical value.

The radiation produced by a microwave generator is to a sufficiently accurate degree plane polarized, coherent, and monochromatic, contrary to light the wavelength of which is smaller by a factor of 10^5 and the radiation of which is most often only quasi-monochromatic. Because of these differences, the analogy between certain optical experiments and the corresponding microwave ones cannot be considered to be exact.

A simple means for theoretically calculating the field, especially in the neighbourhood of the object, would seem to be of value. The Kirchhoff theory has been chosen here even though it is a scalar one. In the following, an attempt to develop and modify this theory so that it can be applied to the case of phase objects will be presented.

A program of research involving the experimental investigation of diffraction patterns of microwaves formed by phase objects was undertaken in this laboratory and the results are reported in this paper. The diffraction fields of dielectric circular plates and of geometrically complementary apertures in screens have been examined and recorded. In all experiments, perspex was used as dielectric material. In order to estimate the influence of the form of the diffracting object, the fields produced by rings and lens-shaped objects have also been recorded.

THEORETICAL SECTION

2. Calculations

The solution of any problem concerning the diffraction of electromagnetic waves by obstacles and apertures requires the solution of Maxwell's equations and the equations for the boundary conditions. Microwave measurements of the diffraction field within and close to apertures and disks have stimulated many theoretical investigations [8, 9, 10, 11]. The simplest problem of this type is the diffraction of electromagnetic waves by a small hole in an infinite plane conducting screen.

Attempts have been made to give a theoretical explanation of the diffraction patterns of various phase objects (Neugebauer [12], Severin [13, 14] and v. Baeckmann [13])—the simplest phase object so far studied being a non-absorbing circular plate with a refractive index different from the surroundings. It has been pointed out by Andrews [1] that the Kirchhoff theory can be used for analysing the near zone. Andrews has compared theoretical predictions of the diffraction field by means of Kirchhoff's theory with experimental values of the intensity along the axes of circular apertures at distances of a few wavelengths and at the aperture itself, and he found that the theory could be satisfactorily used for giving a quantitative interpretation of the field behind a circular aperture in a conducting screen [1, 15]. By proceeding from this theory and introducing some necessary modifications, the author has found it possible to present a theoretical interpretation of the diffraction field.

a) *Kirchhoff's theory of diffraction applied to a hole in a conducting screen*

In the Kirchhoff method, the diffracted field is expressed as a double integral over the aperture. This method is quantitatively fairly accurate in and near the forward direction. Away from this direction, it will, however, be inaccurate owing to its scalar character. In spite of Kirchhoff's incorrect assumption that the intensity over the aperture is the intensity of the undisturbed beam, the method is quite applicable and has moreover been experimentally checked, for microwave measure-

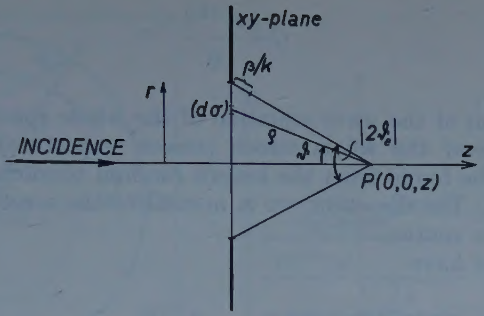

Fig. 1. Schematic representation of the diffracting object (radius r) with respect to the (x, y, z) coordinate system.

ments, by Andrews [1]. The experiments established the fact that the Kirchhoff method is more accurate than commonly supposed.

Andrews has drawn attention to the correctness of Kirchhoff's obliquity factor by performing microwave measurements of intensities at points *on the axis* at a distance from an aperture in a metal screen which was small compared with the diameter of the aperture. A satisfactory quantitative prediction of the positions of the maximum and minimum intensities of the diffraction patterns of a circular aperture not only in the Fresnel region but also behind the aperture and in the plane of the aperture itself has been obtained.

We will consider a thin screen in the plane $z = 0$ of a rectangular coordinate system (Fig. 1). A monochromatic wave, originating from a source in the negative half space ($z < 0$), is assumed to be incident normally opon the screen. Kirchhoff's theory [16] gives the following expression for the amplitude of the diffraction field, at a point $P(x, y, z)$ in space, arising from additive effects from the whole aperture

$$u_P = \frac{i\,u_0}{4\pi}\int\int\left\{k\frac{e^{-i\phi}}{\varrho}(1+\cos\vartheta) - i\frac{e^{-i\phi}}{\varrho^2}\cos\vartheta\right\}d\sigma \tag{1}$$

where u_0 is the amplitude of a plane wave incident normally upon the aperture, k the wave number $k = 2\pi/\lambda$, $d\sigma$ an element of area in the aperture, ϱ the distance from the element $d\sigma$ to P, ϕ the phase lag of the component from $d\sigma$ behind the component from an element at the base of a perpendicular from the point P to the plane of the aperture and ϑ the angle between the incident beam and a line from $d\sigma$ to the point $P(x, y, z)$.

Since the deduction of Eq. (1) is difficult to find in the literature and since misprints occur in other articles [1], we will present here a simple deduction of this important equation:

The Kirchhoff approximation gives from the time-independant scalar eqn.

$$\Delta u + k^2 u = 0$$

the Kirchhoff integral

$$4\pi\,u_P = \int\int\left(u\frac{\partial G}{\partial z} - \frac{\partial u}{\partial z}G\right)d\sigma,$$

where
$$G=\frac{e^{-ik\varrho}}{\varrho}$$

is the Green equation of the wave equation of the whole space and the integral for u_P must be taken over the whole screen (screen + aperture). The wave function u_P at a point P can be found from the known random conditions ($z = +0$) of u and $\partial u/\partial z$ on the screen. The direction $+z$ is normal to the screen $z=0$ in a direction away from the wave source.

In the aperture we have

$$u=\frac{e^{-ik\varrho_0}}{\varrho_0},\qquad \frac{\partial u}{\partial z}=-ik\frac{e^{-ik\varrho_0}}{\varrho_0}\cos(z,\varrho_0).$$

By introducing the values of G and u in the equation for u_P, we get

$$u_P=\frac{e^{-ik\varrho_0}}{4\pi\varrho_0}\int\int\left\{ik\frac{e^{-ik\varrho}}{\varrho}(\cos(z,\varrho_0)-\cos(z,\varrho))-\frac{e^{-ik\varrho}}{\varrho^2}\cos(z,\varrho)\right\}d\sigma$$

Note that the second term in (1) cannot be neglected when ϱ is of the order of a wavelength. Observe also the direction factors $(1+\cos\vartheta)$ and $(\cos\vartheta)$ for each of the two terms.

The field along the axis of the aperture can easily be calculated by integrating (1) over the area of the aperture. We define z as the distance of $P(0, 0, z)$ from the aperture $(0, 0, 0)$ (Fig. 1) and β as the phase of the component coming from the very edge of the aperture. The integration of (1) for a circular aperture yields

$$u_P=u_0\,i\left\{(\sin\beta+i\cos\beta)\left(\frac{\beta+2kz}{2\beta+2kz}\right)-i\right\}. \tag{2}$$

Fig. 2 shows a graphical representation of the amplitude u_P when u_0 has been normalized to unity. Note that the curve is only valid for a fixed z-value. The spiral shape indicates how the amplitude and phase change for different β values. The dashed circle is the asymptote approached by the spiral.

We can also express the amplitude at P in terms of the radius of the aperture by means of

$$\begin{aligned} r/\lambda &= \sqrt{(\beta/2\pi)^2+\frac{z\beta}{\lambda\pi}} \\ \beta &= k\left(\sqrt{z^2+r^2}-z\right) \end{aligned} \tag{3}$$

where r is the radius of the aperture.

b) *Modification of Kirchhoff's theory in order to obtain the field of a phase object*

So far the diffraction patterns of an aperture in a conducting screen have been treated. When working with dielectrics, a modification of the above treatment is necessary.

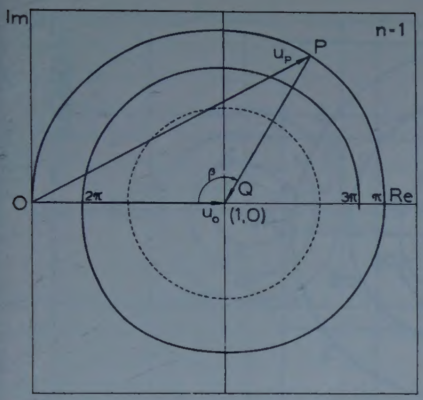

Fig. 2.

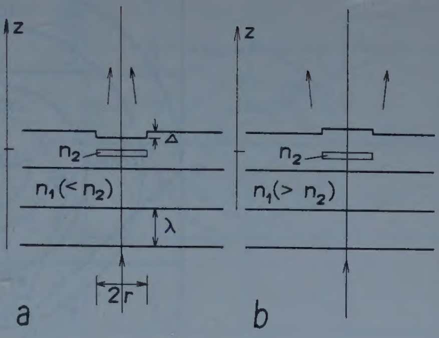

Fig. 3.

Fig. 2. Plots of the complex amplitudes for values of β from 0 to 3π taken at a point 1λ from the center of the aperture on the axis. *OP* represents the field behind the aperture and *PQ* the field for the complementary case—i.e. a disk.

Fig. 3. A phase-changing object, a) denser b) less dense than the surroundings, introduced into a plane wavefront. The transmitted wavefronts produce mainly convergent effects and divergent effects respectively.

A circular phase-changing obstacle (e.g. a dielectric disk) introduced into a plane wave front will because of the difference in the refractive index n_2 from that n_1 of the surrounding area give rise to an optical path difference

$$\Delta = e(n_2 - n_1), \tag{4}$$

where e is the thickness of the obstacle. The corresponding phase difference will be

$$\varphi = -ke(n_2 - n_1) \tag{5}$$

The amplitude at a point $P(x,y,z)$ can for this case be obtained in the following way. Let us interpret $P(0,0,z)$ as a resultant—one part coming from the circular obstacle and the other from the geometrically complementary area extended to infinity. On regarding Fig. 2, it is found that the vector u_P is the amplitude arising from the central disk and, for convenience, we have chosen it as a reference for the phase difference. The undisturbed field is represented by the vector u_0. The optical Babinet's principle, deduced from the Huygens principle, makes it easy to obtain the results for the complementary problem of a circular aperture. Thus, according to this principle, the amplitude of the waves coming from the plane $z = 0$ except for the central disk is represented by $PQ, (u_0 - u_P)$, for the case when the whole field is phase-even.

The intensity distribution along the axis of the circular phase object can easily be calculated and constructed. We must distinguish between two cases: $n_2 > n_1$ (a dielectric disk) and $n_2 < n_1$ (a hole in a dielectric screen).

The two cases are indicated in Fig. 3 where the wavefronts are drawn for n_2 larger and smaller than n_1 respectively. In the first case, it is evident from the general shape of the wavefronts that radiation will be concentrated towards the axis region

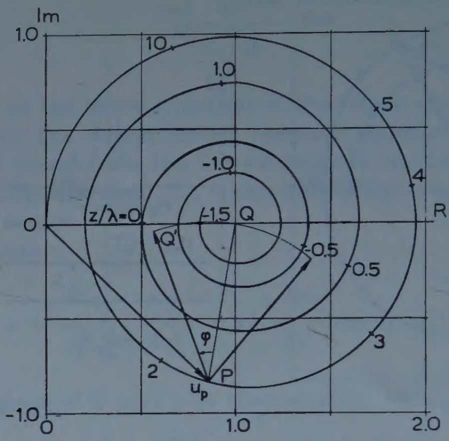

Fig. 4. Spiral representing the amplitude and phase along the z-axis for a circular aperture ($r = 2\lambda$) in a conducting screen. The undisturbed field amplitude has been normalized to unity. Values for z/λ are marked along the curve. OP is the field behind the aperture, PQ the field behind the corresponding disk and PQ' the field behind the same disk when the external area differs in phase by φ from that in the case PQ.

in the direction of propagation. In the geometrically complementary case, we have the opposite effect.

Eq. (2) may be rewritten in the following form in order for it to be more suited for our purpose:

$$u_P = u_0\, i\, \{(\sin\beta + i\cos\beta)\, \tfrac{1}{2}(1 + \cos\vartheta_e) - i\} \tag{6}$$

where $\beta = k\,(\sqrt{z^2+r^2} - z)$, r is the radius of the disk and $\cos\vartheta_e = z/\sqrt{z^2+r^2}$.

By introducing polar coordinates (ϱ, ψ), we get Eq. (6) in the form

$$u_P/u_0 = 1 - \varrho\, e^{-i\psi} \tag{7}$$

which gives u_P as a function of z and r.

In Eq. (7) $\quad \varrho = \frac{1}{2}\left(1 + z\sqrt{z^2+r^2}\right)$ and $\psi = \varphi$.

In Fig. 4, the imaginary components of the amplitude are plotted versus the real components (Eq. 7) for varying z values and r constant ($r = 2\lambda$). We thus get a survey of the field along the axis of an aperture in a completely conducting screen. In Fig. 4 and the other spiral-shaped figures, the patterns are normalized to the intensity of the incident, plane unperturbed wave (denoted by the subscript u_0).

If the external area differs in phase by an amount φ, then this is equivalent to a turning of the vector PQ (Fig. 4) through an angle φ. For a dielectric disk in air, the component corresponding to the external area is phase-displaced before the resultant from the central plate and therefore the vector PQ is turned in the positive direction. The amplitude at P of the diffraction pattern proceeded from a circular phase-changing obstacle is represented by OQ' in Fig. 4.

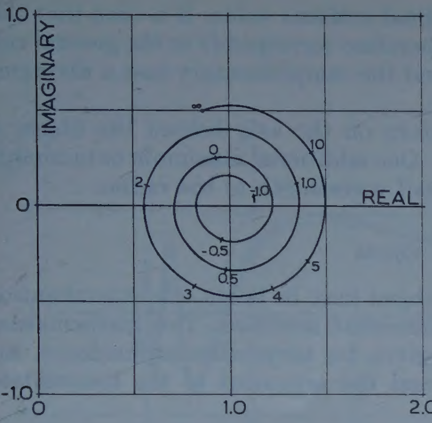

Fig. 5.

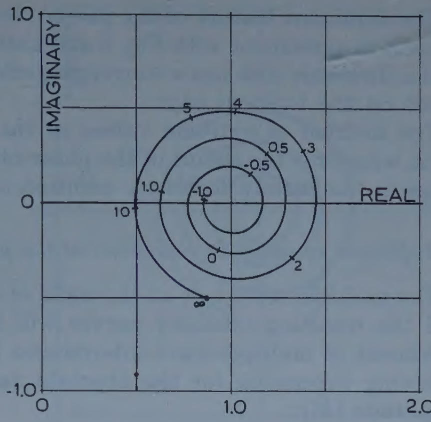

Fig. 6.

Fig. 5. Plots in complex space to express amplitudes and phases at points (denoted by values for z/λ along the curve) on the axis of a dielectric disk ($r = 2\lambda$, $\varphi = +30°$).

Fig. 6. Plots in complex space to express amplitudes and phases at points (denoted by values for z/λ along the curve) on the axis of an aperture in a dielectric screen ($r = 2\lambda$, $\varphi = -30°$).

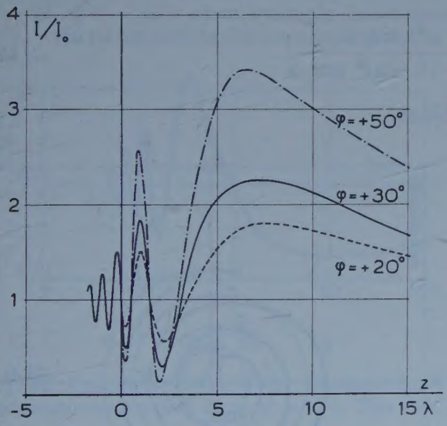

Fig. 7.

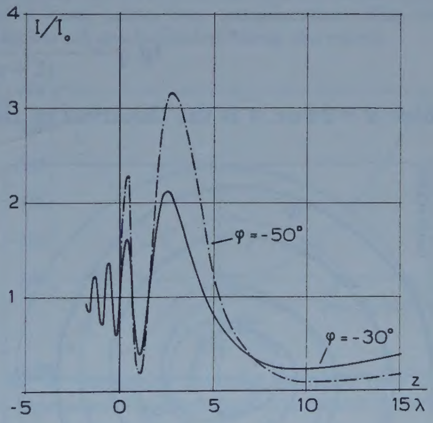

Fig. 8.

Fig. 7. Calculated intensities, along the axis, of diffraction patterns behind dielectric disks ($r = 2\lambda$).

Fig. 8. Calculated axial distributions of the diffraction field of apertures ($r = 2\lambda$) in dielectric screens.

If the construction according to Fig. 4 is performed in order to get the diffraction field, we obtain Figs. 5 and 6. These figures show the amplitude spiral corresponding to an optical path difference equal to $+\lambda/12$ and $-\lambda/12$ respectively.

The intensity distribution along the axis is found by squaring the amplitudes. In Figs. 7 and 8, I/I_0 is plotted vs the distance z from the object. I_0 represents, in analogy with the previous subscript usage, the intensity of the unperturbed beam at the corresponding z-value.

The dominant feature of the pattern is the final extreme value. It is seen that this value is in agreement with Fig. 3 and that it therefore corresponds to the general rule that a dielectric disk has a converging effect and the complementary case a diverging effect on the incident rays.

The number of extreme values in the pattern on the axis behind the object is $2r/\lambda$, where r is the radius of the phase object. One additional maximum or minimum arises in the pattern for every addition of a half wavelength to the radius.

c) *Influence of multiple reflexions at the phase objects*

The multiple reflexions at the walls of the object may be taken into consideration and the resulting intensity curves will be somewhat modified. The mathematical treatment of multiple-wave interference [17] gives, for perpendicular incidence, the following expression for the absolute value and the argument of the transmitted amplitude (E_t):

$$\left(\frac{E_t}{E_0}\right)\left(\frac{E_t}{E_0}\right)^* = \frac{4n^2}{4n^2 + (1-n^2)^2 \sin^2(\alpha/2)}$$

$$\left|\frac{E_t}{E_0}\right| = \frac{2n}{\sqrt{4n^2 + (1-n^2)^2 \sin^2(\alpha/2)}} \tag{9}$$

$$\operatorname{tg}\varphi = -\frac{(1-n^2)\sin\alpha}{(1+n)^2 - (1-n)^2\cos\alpha} \tag{10}$$

where $\alpha = 2kne$. e is the thickness of the object.

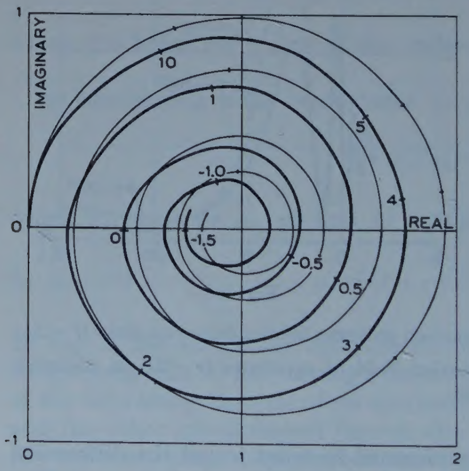

Fig. 9.

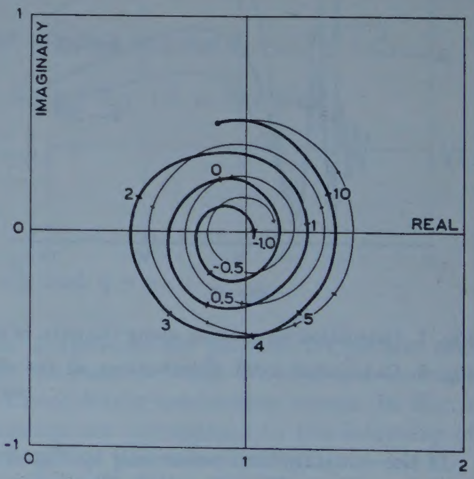

Fig. 10.

Fig. 9. Modification of Fig. 4. Plots in complex space obtained when the multiple reflexions are taken into account.

Fig. 10. Spiral obtained for the amplitude and phase along the axis of a dielectric plate ($r = 2\lambda$, $\varphi = +30°$) when multiple interferences have been taken into consideration. The thin curve represents the uncorrected curve. Values for z/λ are indicated along the curve.

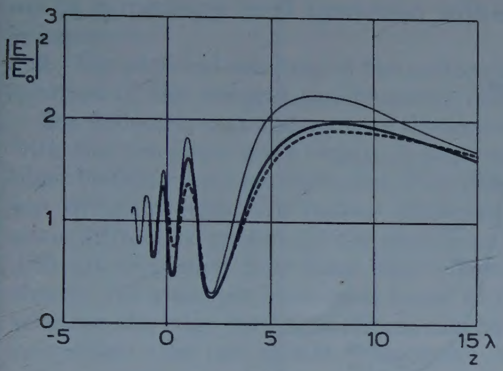

Fig. 11.

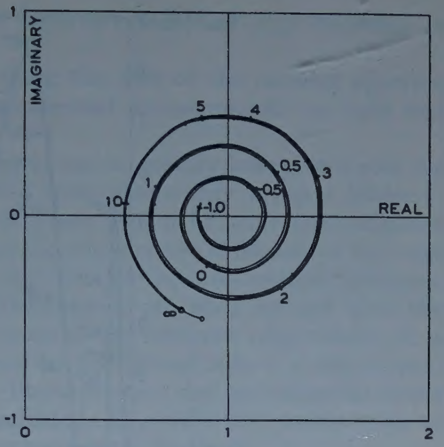

Fig. 12.

Fig. 11. Calculated intensities, obtained from Fig. 10, of diffraction patterns behind a dielectric disk ($r = 2\lambda$, $\varphi = +30°$). The thin curve represents the uncorrected theoretical curve and the dashed curve the experimental curve.

Fig. 12. Spiral obtained for the amplitude and phase along the axis of a hole in a dielectric screen ($r = 2\lambda$, $\varphi = -30°$) when multiple interferences have been taken into consideration. The thin curve represents the uncorrected curve. Values for z/λ are indicated along the curve.

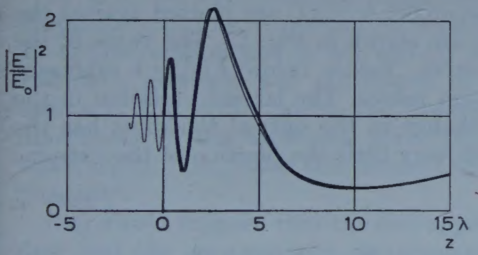

Fig. 13.

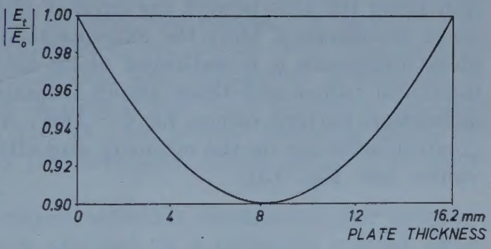

Fig. 14.

Fig. 13. Calculated intensities, obtained from Fig. 12, of diffraction patterns behind a hole in a dielectric screen ($r = 2\lambda$, $\varphi = -30°$). The thin curve represents the uncorrected theoretical curve.

Fig. 14. Calculated transmission factor $|E_t/E_0|$ for a perspex plate as function of the plate thickness.

Fig. 9 gives a representation of these values in the complex plane. The spiral is somewhat displaced when these reflections are taken into account. The construction of Figs. 10, 11, 12 and 13 was carried out in agreement with the construction used in 2.b. The largest changes are in the pattern of the dielectric plate where all extreme values are somewhat smoothed out. Fig. 14 shows how $|E_t/E_0|$ changes with the thickness of the dielectric material.

d) *Influence of the optical thickness on the shape of the pattern*

Fig. 15 shows the influence of the optical path difference on the appearance of the field. In this Fig., the height and position of the extreme values of the field distribu-

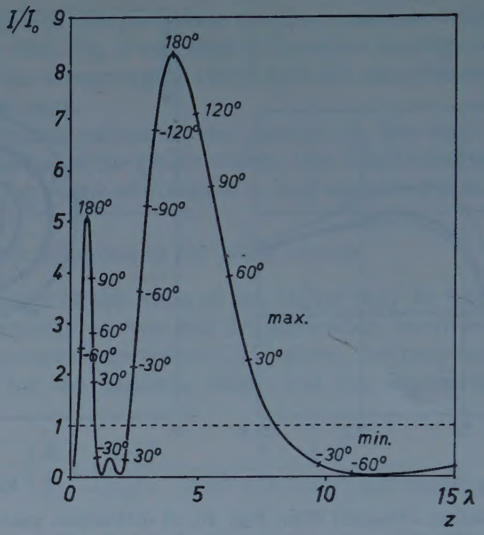

Fig. 15. Heights and positions of maxima and minima in the diffraction pattern along the axis of a circular phase object ($r = 2\lambda$). Values of the parameter φ (phase difference) are indicated along the curve.

tion along the axis behind the circular phase object ($r = 2\lambda$) are plotted against the space coordinate z. Only the extreme points are shown in Fig. 15. The value of the phase difference φ is indicated along the curve. Values below $I / I_0 = 1$ represent minimum values and those above 1 maximum values. The largest variation in the diffraction pattern occurs for $\varphi = 180°$. A change in the optical thickness has the greatest influence on the intensity and effects very little the position of the extreme values (see Fig. 15).

e) *Vector theory with respect to the simple Kirchhoff-Fresnel scalar theory*

The function in the Kirchhoff formula is, however, a scalar wave function satisfying the wave equation. The diffraction field at a point in space has amplitude and phase, but it is not a vector field.

The $\bar{E}$-and $\bar{H}$- field patterns are not quite coincident in the very neighbourhood of the aperture plane, but with increasing distance from the object the distributions become more nearly coincident and in the far-zone region the dominant parts of the field vectors have a plane wave relationship.

Because of this, the classical Kirchhoff-Fresnel theory, which is unable to take into account the polarization of the waves, will not give, strictly speaking, the intensity distribution of the field (obtained by the Poynting vector) in the near-zone.

Kirchhoff's scalar theory has been used with success for studying the diffraction field behind dielectric objects penetrated by a plane, normally incident electromagnetic wave. As will be seen later, we have obtained a fairly good agreement between theory and experiment. Only in the very neighbourhood of the object do the variations in the field fall below the theoretical amplitudes.

Kirchhoff's theory of diffraction seems to be convenient and it is desirable to give increased attention to it since:

1. The results obtained for the intensity along the axis of the circular aperture are in surprisingly good agreement with experimental measurements on light and microwaves.

2. The physical meaning of the surface integral can be readily interpreted and the solution of the integral can be easily obtained from elementary integral tables.

For dielectric materials, where the screen thickness cannot be neglected compared with the free space wave length, it is questionable whether the thickness of the edge must be taken into consideration. Two phase objects with the same optical thickness, but different refractive indices (different thicknesses), probably do not give the same diffraction pattern in the near zone because of the different edge effects. It is difficult to predict how these edge effects can be introduced into a mathematical theory. No attempts have been found in the literature and also no comments about whether the edge thickness effects can be neglected. This difficulty would seem to necessitate that one should concentrate on experimental findings.

In microwave experiments, the radiation produced is plane polarized, coherent and monochromatic and the electrical conditions (polarization effects) are not constant around the edge of the object. Here, however, a vector treatment would seem more convenient but at the same time even more difficult. Instead of considering the phase difference as a step alteration, one could treat the change as a continuous transition, from the front edge of the object to the back edge, in the direction of propagation.

In 2. b, we have used the scalar Babinet's principle which is deduced from the Huygens' principle. However, we must keep in mind that Kirchhoff's theory is only an approximation and is not strictly applicable to our vector field. This form of Babinet's principle was postulated in connection with diffraction phenomena in ordinary light optics where the distances of field points from the object and the dimensions of the apertures were large, viz. at least several thousand times the wavelength. The scalar diffraction theory [18] supplies a simple proof of Babinet's principle.

One would suppose that the two approximate solutions constructed (the dielectric disk and the geometrically complementary aperture in a dielectric screen) would obey Babinet's principle. It is possible to convert Babinet's principle to a rigorous solution of the electromagnetic diffraction problem (a rigorous proof for the electromagnetic case has been obtained by Copson [19] and Meixner [20]) when the diffracting obstacle and the complementary screen are plane and completely conducting. Using this principle, the electromagnetic field at every point for one diffracting problem can be found from the known complementary field by $\bar{E}\rightarrow\bar{H}$ and $\bar{H}\rightarrow-\bar{E}$.

In the following, a short survey of a generalized version of the last-mentioned Babinet's principle is discussed which holds for holes in a screen and plane plates consisting of dielectric material.

The rigorous formulation of Babinet's principle for perfect conductors [19, 20] can be extended and generalized to absorbing and transparent materials [21]. It is only possible to derive Babinet's principle in an approximate form for screens that are not perfect conductors.

The electromagnetic field incident on a phase object can be split up into three parts—the first part passes through undiffracted, the second part is diffracted as though the screen were a perfect electrical conductor and the third part is diffracted as though the screen were a perfect magnetic conductor.[1] By calculating each of these parts separately, it is possible to compute the diffraction field.

Babinet's principle can be generalized in the following way [21]:

If an electromagnetic field $E_x = E_0 e^{-ikz}$ is incident perpendicularly on a plane, infinitely thin plate whose reflection and transmission properties are characterized by the factors Z and T, respectively, then the diffraction field in front[1] of the plate can be computed as though the fraction $TE_0 e^{-ikz}$ passed undiffracted and as though the fraction $\frac{1}{2}(1+Z-T)E_0 e^{-ikz}$ were diffracted by a complementary hole in a plane thin screen which is a perfect magnetic conductor and as though the fraction $\frac{1}{2}(1-Z-T)E_0 e^{-ikz}$ were diffracted by the same hole in a screen which is a perfect electric conductor. An analogous statement will hold for a perforated screen.

EXPERIMENTAL SECTION

3. Apparatus and experimental procedure

A full-space arrangement with an incident wave which is practically a linearly polarized plane wave was used. The apparatus used (Fig. 16) was designed in order to eliminate the possibility of interaction between the objects studied and the apparatus required for diffraction measurements. Care was taken to protect the system from scattered radiation from nearby objects. The linear proportions of the apparatus were chosen so that disturbing reflexions from the ground were a minimum and so that the object was subject to a homogeneous plane wave. Ground reflexions become serious as the distance from the diffracting obstacle is increased—they cause fluctuations in the amplitude in the incident field and are a disturbing factor on the incident side. In order to reduce reflexions, the apparatus was set up out of doors on a copper-covered roof (Fig. 17). Measurements were only performed during absolute calmness. No disturbing reflexions from the roof could be observed. The measuring equipment and power supplies were located in a field-free space at a considerable distance from

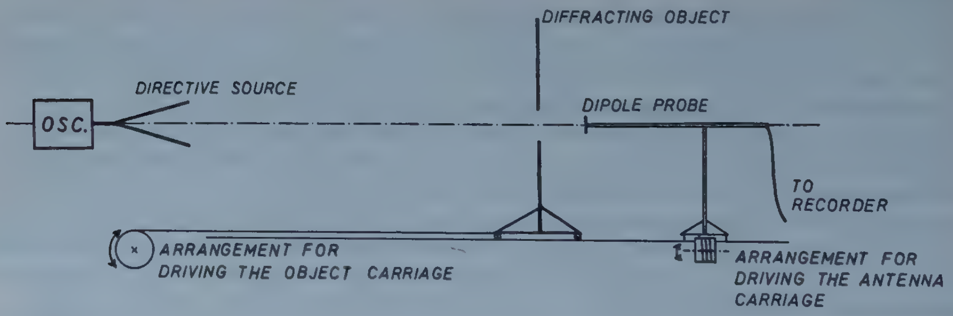
DIFFRACTING OBJECT
DIRECTIVE SOURCE
OSC.
DIPOLE PROBE
TO RECORDER
ARRANGEMENT FOR DRIVING THE OBJECT CARRIAGE
ARRANGEMENT FOR DRIVING THE ANTENNA CARRIAGE

Fig. 16. Arrangement of apparatus for the study of the diffraction pattern produced by a circular phase object.

---

[1] The rigorous formulation of Babinet's principle may be interpreted in the following way: If an electromagnetic field is incident on a perforated, perfectly conducting, infinitely thin screen, the perturbation field in front of the screen is the same as that caused by complementary plates of a material which is a perfect magnetic conductor. The perturbation fields behind the screen and plates are also the same—except for the signs, which are opposite.

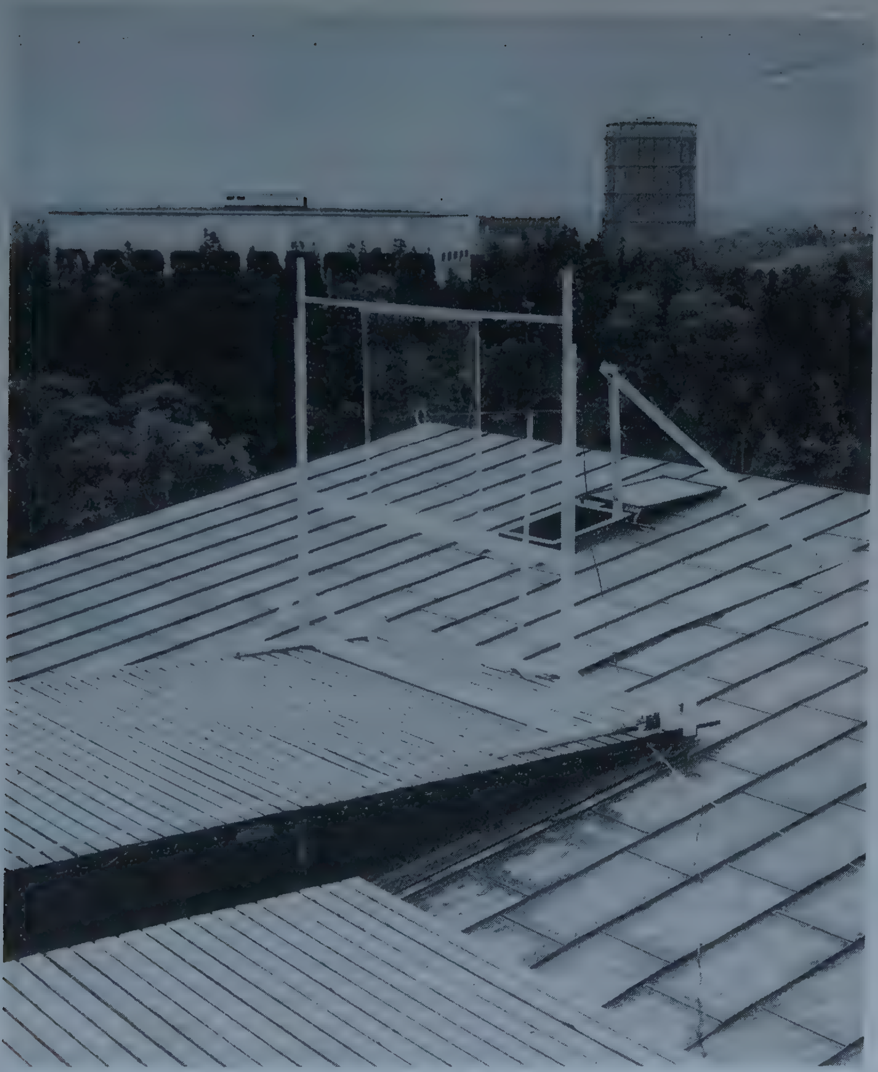

Fig. 17. General view of the object and detector parts of the apparatus.

the apparatus in order to minimize the preturbations. Consequently, long connecting cables were required and this gave rise to erratic results which, however, not particularly pronounced for these measurements of the amplitude.

In the theoretical treatment of the diffraction problem, it is assumed that the incident field is an infinite, homogeneous plane wave. It is, therefore, desirable to approach this type of illumination as closely as possible practically. The dimensions of the apparatus were: The distance between the source and the probe when the latter was situated on the axis of propagation was 1080 cm. The axis of propagation,

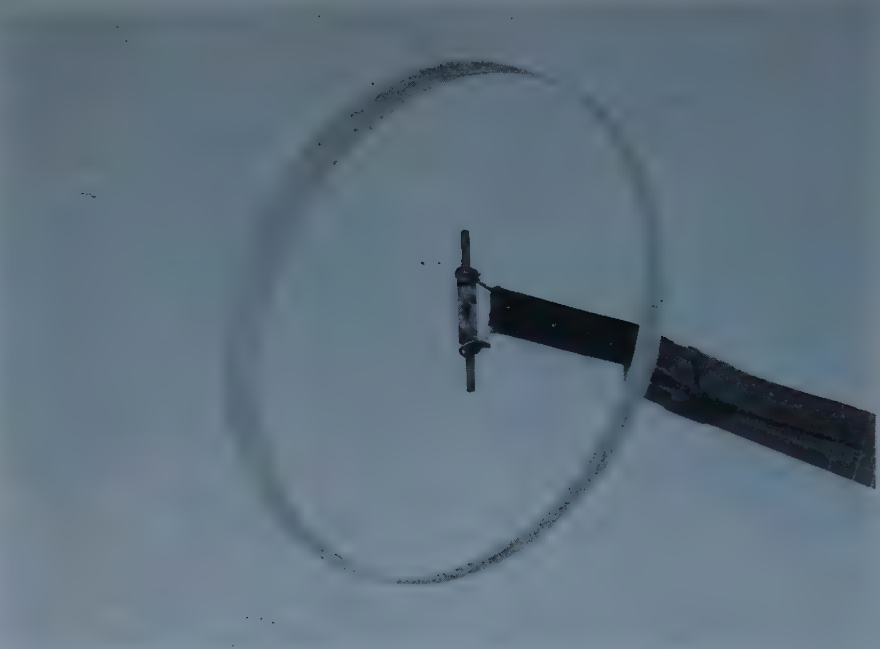

Fig. 18. The probe. The connecting leads to the recorder.

170 cm above a wooden floor on the roof, was horizontal and the field ($\bar{E}$ field) plane polarized vertically.

The measurements have all been concentrated on the field distributions in planes parallel to the coordinate axis in Fig. 1 for the case of a wave incident normally on the diffracting structure. In the study of the aperture fields, the screen must be large enough to represent a practical realization of an infinite screen, i.e. the effect of diffraction by the edges of the screen must be negligible in the region of the aperture field.

A 5.15 cm wave (5850 Mc/s) was produced with a Leybold magnetron oscillator (Magnetron type MG 20, Deutsche Elektronik GmbH). An impulse with a duration of 1/150 sec. is obtained every 1/50 sec.

As detector, a germanium diode, which was considered to be a square-law detector, was used in order to measure relative field intensities directly.

Thin brass tubes were fixed to the ends of the diode (see Fig. 18) in order to obtain a simple dipole antenna ($\lambda/2$ antenna). The diode was connected by means of a cable which was led from the probe along a wooden rod away from the source of radiation in the propagation direction (Fig. 16). The cable was then led down to the floor and to the input of a recording potentiometer.

The probe assembly consists of a wooden carriage (Fig. 17) which permits a translation of the probe along a direction parallel to the screen and perpendicular to the optical axis. The probe was driven by a synchronous motor at the rate of two wavelengths per minute. The intensities were recorded on a recording potentiometer (Varian G 10) with a sensitivity of 10 mv (0.2 μamp) full scale and a period of 1 sec.

The diffracting objects were mounted on a wooden frame (Fig. 17) which could be moved along rails parallel to the axis of propagation. A synchronous motor, a reduction gear, a drum, a steel wire, and a counterweight served to drive the object carriage parallel to the propagation direction at about 1 mm per sec. The minimum distance from the surface of an object to the center of the probe was limited, by the radius of the probe cartridge, to about 2 mm. A positive and uniform drive was obtained and the object carriage could be moved in either direction along the track.

Disks of various diameters of the dielectric material, viz. perspex with thicknesses of 12, 8, and 5 mm and apertures with various diameters in perspex screens (128 × 128 cm²) with thicknesses of 12 and 4 mm have been examined.

4. Dielectric material used, and its dielectric constant

The dielectric constant of perspex at 5850 Mc/s (the oscillator frequency) was determined in the following way:

For the TE_{01} wave [22] in a rectangular wave-guide, the wavelength Λ in the wave-guide is

$$\Lambda = \frac{\lambda_0}{\sqrt{1-\lambda_0^2/(4\,b^2)}} \tag{11}$$

where $\lambda_0 = c/f$ and b is the width of the wave-guide. For the case where the wave-guide is filled with a dielectric material with the dielectric constant ε, we have

$$\Lambda_\varepsilon = \frac{\lambda_0}{\sqrt{\varepsilon-\lambda_0^2/(4\,b^2)}}. \tag{12}$$

The limiting wavelength in the two cases is $\lambda_0 = 2b$ and $\lambda_0 = \sqrt{\varepsilon}\cdot 2b$.

One method for measuring ε for a low-loss material is to fill the whole wave-guide with the dielectric material (short-circuit measurement) [23] and then measure Λ_ε along a slot in the middle of the long side of the wave-guide by directly measuring the distance between two minima of the standing wave. Λ is also measured without any dielectric material being placed in the wave-guide. ε is obtained in the following way

$$\varepsilon = \frac{\Lambda^2}{\Lambda_\varepsilon^2}\cdot\frac{\Lambda_\varepsilon^2+4\,b^2}{\Lambda^2+4\,b^2}. \tag{13}$$

In the above mentioned method, $\lambda_0 < 2b$. If $\lambda_0 > 2b$, then λ_0 must be measured by frequency measurement, i.e. ε is obtained from

$$\varepsilon = \frac{\lambda_0^2}{\Lambda_\varepsilon^2} + \frac{\lambda_0^2}{4\,b^2}. \tag{14}$$

The thickness of the dielectric plate was 12 mm and this meant that it was most suitable to measure in a standard wave-guide for the 3-cm band (dimensions: 10 × 23 mm²). The wavelength, 5.15 cm, is larger than $2b = 46$ mm but smaller than $\sqrt{\varepsilon}\,2b \approx 73$ mm ($\varepsilon \approx 2.5$). From this, we conclude that λ_0 must be measured with a 6-cm band wave-guide (22 × 47 mm²).

Apparatus used in the measurements:

Signal-generator:	Hewlett-Packard SHF-oscillator Type 670GM (klystron)
Detector:	Indicator amplifier, Sivers Lab. Type S.L.5400
Standing wave meter:	Sivers Lab. S.L.5550/1 (6-cm band) and Sivers Lab. S.L.5341/1 (3-cm band)

Measurements ($b = 4.75$ cm).

Oscillator frequency Mc/s	(λ_0) cm	Λ cm	λ_0 obtained from (11) cm	Λ_ε cm	ε
5900	5.08	5.96	5.05	4.39	2.54
5850	5.13	6.04	5.09	4.45	2.53
5800	5.17	6.10	5.14	4.52	2.54

From these measurements, we find $\varepsilon = 2.54$ at 5850 Mc/s and the refractive index $n = 1.59$.

5. Experimental results

The experimental results are presented in the following. The intensity ratio I / I_0, used as ordinate in the field representations, is equal to the square of the modulus of the electric field E normalized to the incident field at the same point. Here are two methods for recording the diffraction field: (a) the object is held in a fixed position and the field is measured by moving the probe or (b) the object is moved and the probe fixed. In the latter method, the amplitude reduction (which has been measured without the object) must be taken into account.

The diffraction field was examined along the normal through the centre of the object by driving the object carriage by means of the motor. The field was examined by translation of the detector along straight lines in planes behind the phase-changing objects.

Experimentally, I and I_0 are ordinates of a given curve at each displacement as measured directly from the recorder chart. The experimental values from the recordings along the axis are averages obtained from measurements of two chart records in each case. A reproducibility within 5 % was obtained for five recordings taken on different occasions.

Free-space measurements were made with the diffracting objects (disks and apertures in screens) removed, in order to determine the undisturbed field and to get an idea of the planeness of the incident wave. It was found that, over an area as great as that which was examined in the experiments, the power was practically constant and did not fluctuate by more than ± 5 % about the mean level. This fluctuation comes from a weak overlapping field arising from the wooden frame supporting the objects. However, this field was not inconvenient for the measurements since it was weak and always controllable.

The origin is at the intersection of the object plane, taken as the xy-plane (See Fig. 1), and the z axis which is in the direction of the incident field propagation (horizontal). The probe runs were made in the yz-plane parallel to the horizontal y axis. In some cases, measurements were also performed in planes parallel to that of the screen (i.e. the xy-plane), at various distances z, from $z = 0$ (aperture field measurements) to $z = 20\ \lambda$. The field distributions were examined in the plane known as the E plane, the scan being made perpendicular to the direction of the initial incident polarization.

a) *Dielectric circular plate*

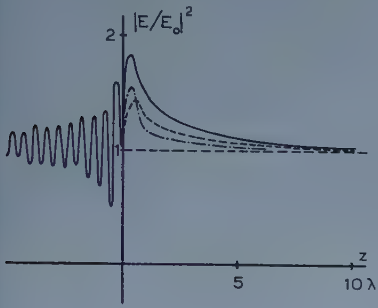

Rec. 1.

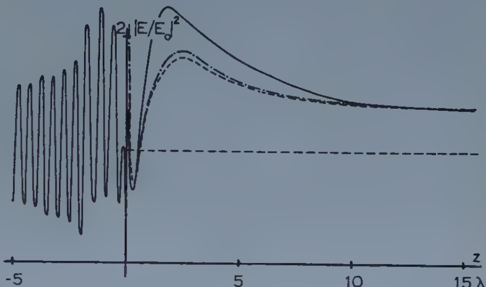

Rec. 2.

Record 1. Dielectric plate. $r = \lambda/2$. Plate thickness: ——— 12 mm, —·—·— 8 mm, – – – 5 mm

Record 2. Dielectric plate. $r = \lambda$. Plate thickness: ——— 12 mm, —·—·— 8 mm, – – – 5mm

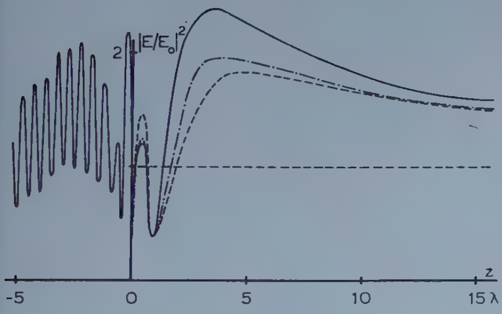

Rec. 3.

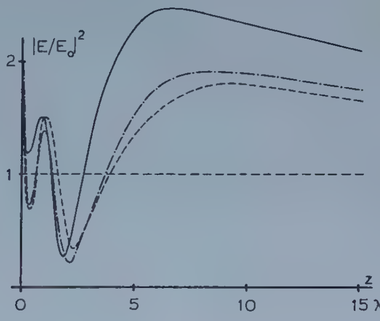

Rec. 4.

Record 3. Dielectric plate. $r = \frac{3}{2}\lambda$. Plate thickness: ——— 12 mm, —·—·— 8 mm, – – – 5 mm.

Record 4. Dielectric plate. $r = 2\lambda$. Plate thickness: ——— 12 mm, —·—·— 8 mm, – – – 5 mm.

In Recordings 1–4, the measurements of the axial distributions of the diffraction fields of dielectric disks are shown for a sequence of diameter sizes. Three different thicknesses 12, 8, and 5 mm were used. The pattern in front of the disks was only recorded for the 12 mm plate.

In addition to the above mentioned field measurements, the near-zone field distributions of the 12 mm plates were also recorded (Recs. 5 and 6) for distances z (planes parallel to that of the plate) at fixed positions between zero and ten wavelengths.

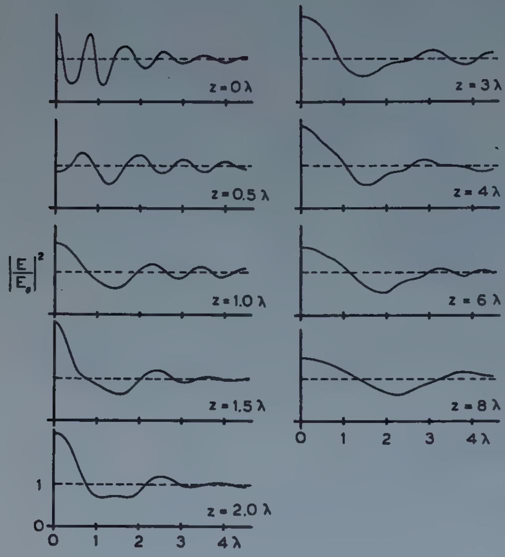

Rec. 5.

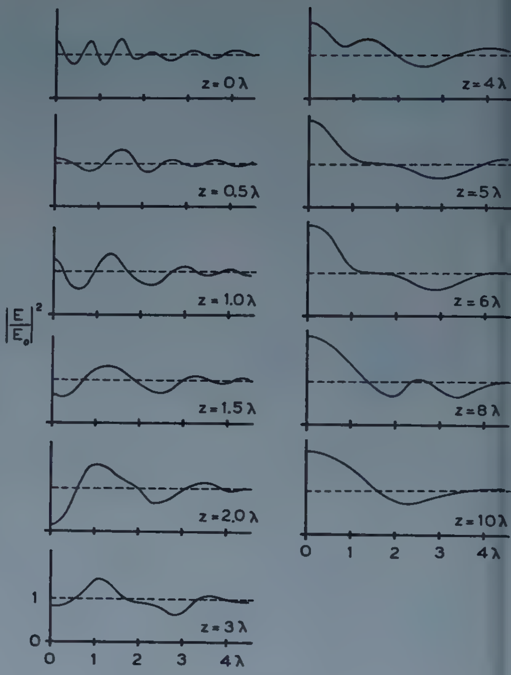

Rec. 6.

Record 5. Dielectric plate. $r = \lambda$. Plate thickness = 12 mm.

Record 6. Dielectric plate. $r = 2\lambda$. Plate thickness = 12 mm.

b) *Circular apertures in a dielectric screen*

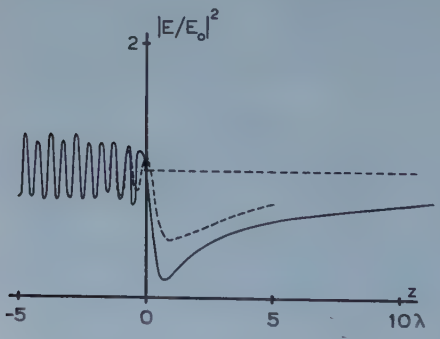

Rec. 7.

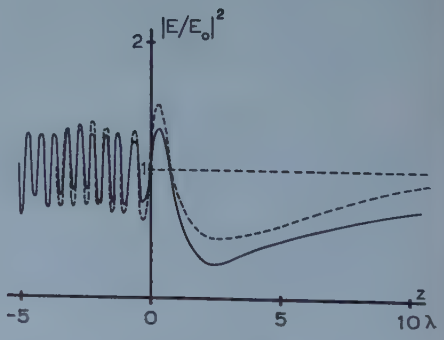

Rec. 8.

Record 7. Aperture in a dielectric screen. $r = \lambda/2$. Screen thickness: ——— 12 mm, – – – 4 mm.

Record 8. Aperture in a dielectric screen. $r = \lambda$. Screen thickness: ——— 12 mm, – – – 4 mm.

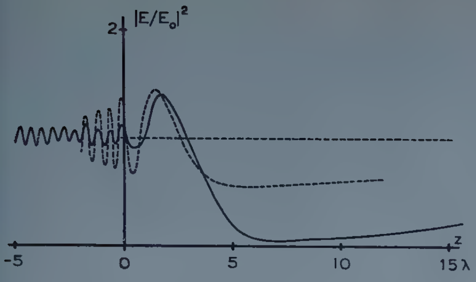

Rec. 9.

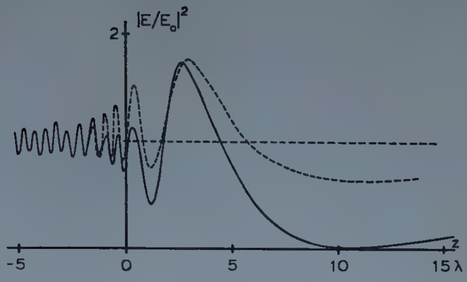

Rec. 10.

Record 9. Aperture in a dielectric screen. $r = \frac{3}{2}\lambda$. Screen thickness: ——— 12 mm, – – – 4 mm.

Record 10. Aperture in a dielectric screen. $r = 2\lambda$. Screen thickness: ——— 12 mm, – – – 4 mm.

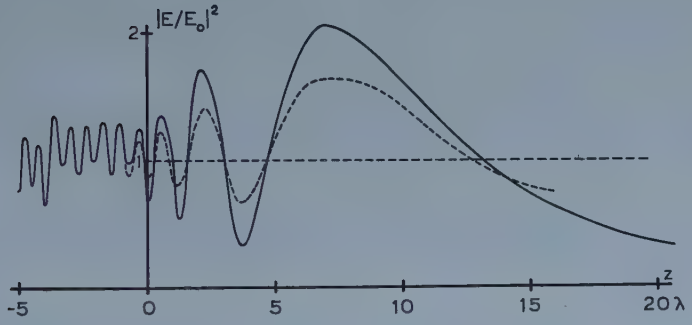

Record 11. Aperture in a dielectric screen. $r = 3\lambda$. Screen thickness: ——— 12 mm, – – – 4 mm.

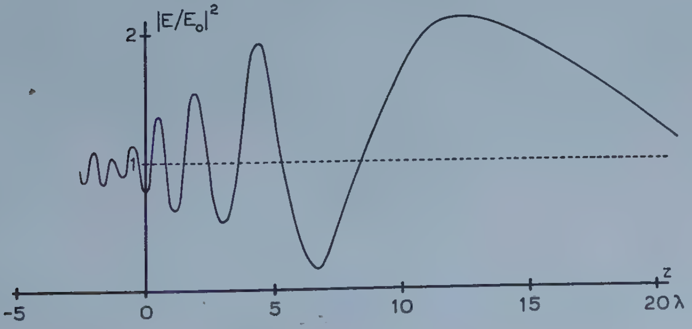

Record 12. Aperture in a dielectric screen. $r = 4\lambda$. Screen thickness = 12 mm.

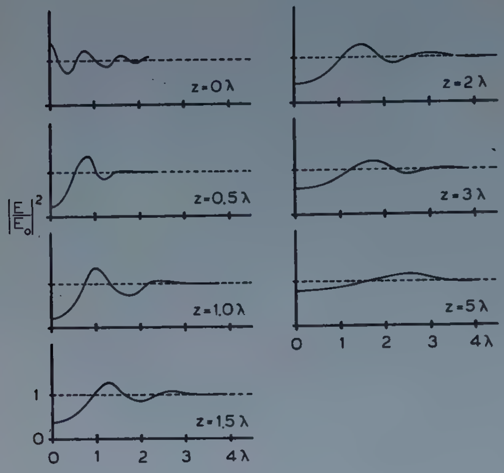

Rec. 13.

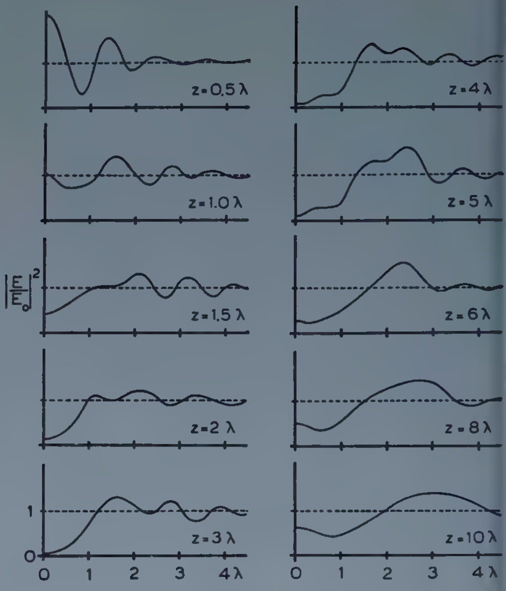

Rec. 14.

Record 13. Aperture in a dielectric screen. $r = \lambda/2$. Screen thickness = 12 mm.

Record 14. Aperture in a dielectric screen. $r = \lambda$. Screen thickness = 12 mm.

In Recs. 7–12, the field distribution along the aperture axis for circular apertures of intermediate sizes, $d = \lambda$ to $d = 8\lambda$, are shown. Two screen thicknesses, 12 and 4 mm, were used.

For the 12 mm screen, measurements were also performed in planes parallel to the screen at various distances z from $z = 0$ (aperture field measurement) to $z = 20\lambda$. These recordings were made for aperture sizes from $d = \lambda/2$ to $d = 4\lambda$ and are reproduced in Recordings 13–15.

c) *Paraffin lens inserted in the aperture of a dielectric screen*

A paraffin lens with a maximum thickness of 25.2 mm and an edge thickness of 12.0 mm was fitted into the 4λ aperture of the 12 mm dielectric screen. Recs. 16 and 17 show the pattern along the axis together with measurements performed in planes parallel to that of the screen at the same z distances as those for the measurements of the field of an aperture 4λ in diameter.

d) *Dielectric ring*

The diffraction patterns of dielectric rings (8 mm thick) were recorded as in the preceding measurements. Recs. 18 and 19 show patterns from rings with an external diameter of 3λ and an interior diameter of 1λ and 2λ.

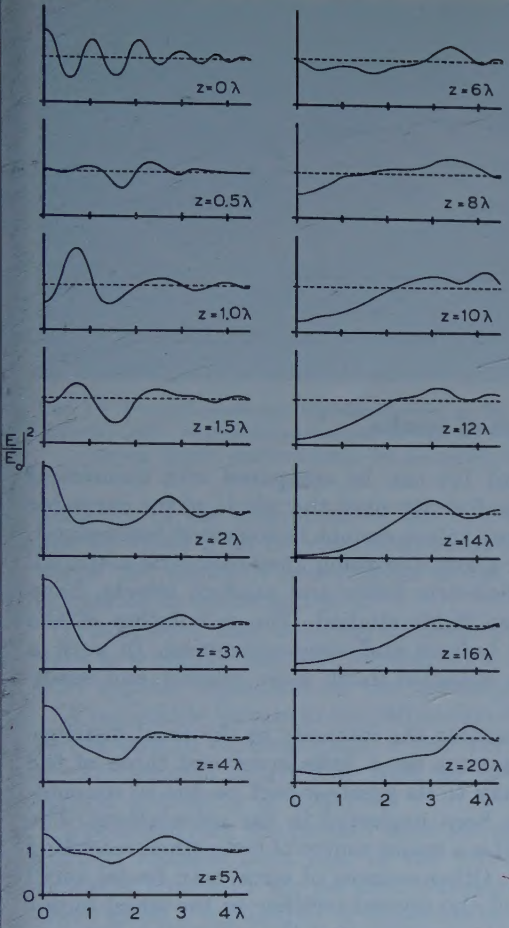

Rec. 15.

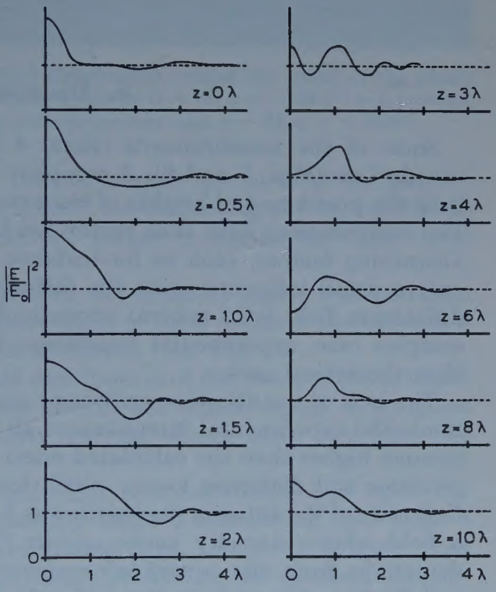

Rec. 16.

Record 15. Aperture in a dielectric screen. $r = 2\lambda$. Screen thickness = 12 mm.

Records 16 and 17. Paraffin lens inserted in the aperture of a dielectric screen. $r = 2\,\lambda$.

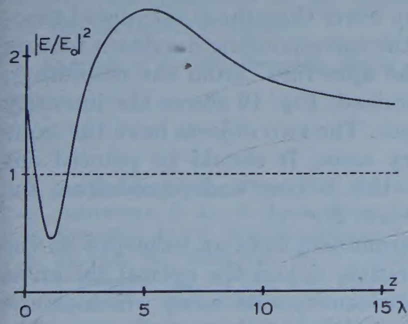

Rec. 17.

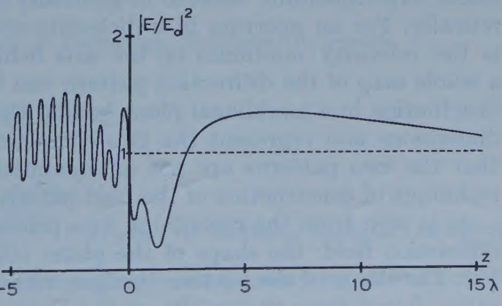

Rec. 18.

Record 18. Dielectric ring. External radius = $\frac{3}{2}\lambda$. Interior radius = $\lambda/2$. Thickness of the ring = 8 mm.

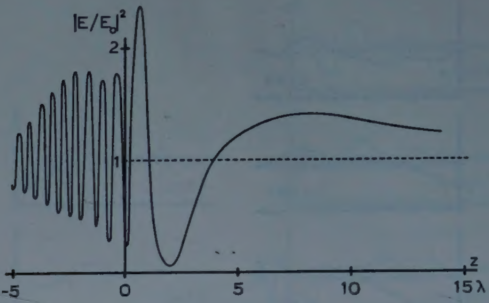

Record 19. Dielectric ring. External radius = $\frac{3}{2}\lambda$. Interior radius = λ. Thickness of the ring = 8 mm.

6. Discussion of results

Some of the measurements (Recs. 4 and 10) can be compared with theoretical calculations (Figs. 7 and 8). A complete conformity over the whole of the curve for both the positions and heights of the extreme values cannot be expected beforehand. The computations have been performed for a non-absorbing ideal dielectric material. Disturbing factors, such as for instance dielectric losses and random effects, have only a small influence upon the diffraction fields studied. The calculation of the diffraction field is in general exceedingly tedious and time-consuming. In such a complex case, experimental results can be obtained much more quickly and easily than theoretical ones.

The lack of quantitative agreement concerning the intensity in the axial distributions (the experimental intensities of all maxima are a little lower and those of the minima higher than the calculated ones) may to its greatest part be due to inhomogeneities and dielectric losses, which have been neglected in the calculations. The finite size of the antenna (its length was $\lambda/2$) is a major source of error when recording a field whose intensity varies rapidly [2]. Other sources of error may be (a) small deviations from the square-law response of the crystal rectifier to the small imput and (b) disturbances from the cables. It is also possible that the interaction between the probe and the phase object might account for part of the disagreement. In addition, a possible depolarization effect from the aperture may occur.

The results show that a predominant characteristic of the diffraction pattern of a dielectric disk is the peak of intensity on the axis behind the object. The peaks found experimentally seem to be generally slightly lower than those calculated theoretically. For an aperture in a dielectric screen, the corresponding dominant feature is the intensity minimum on the axis behind the apterture. From the recordings, a whole map of the diffraction pattern can be obtained. Fig. 19 shows the intensity distribution in a meridional plane behind the object. The two objects have the same dimensions and represent the two complementary cases. It should be pointed out that the two patterns are not antisymmetrical—this is best understood from the technique of construction of the field pattern (See sec. 2.).

As is seen from the recordings, two primary parameters have an influence on the diffraction field: the shape of the phase object (radius r) and the optical thickness (Δ). The shape of the pattern changes with r in conformity with a law which can be easily found from the results of the large number of experiments performed. The

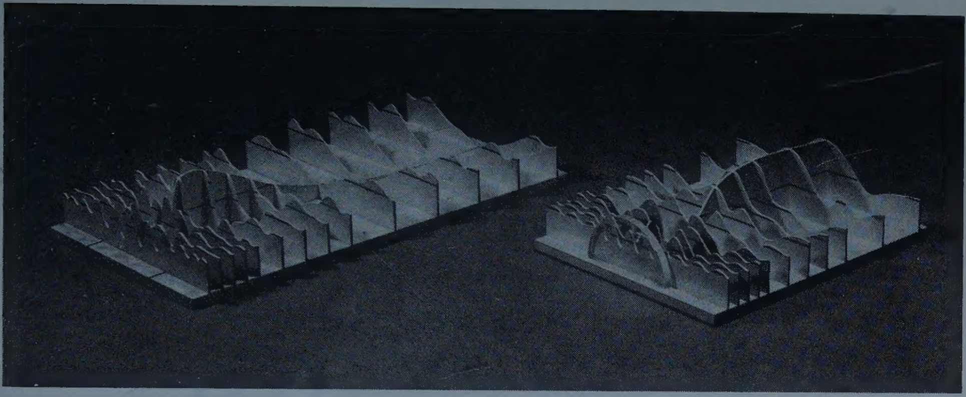

Fig. 19. Two-dimensional representation of the field distribution behind the plane of the phase objects. Left—intensity variations caused by a circular aperture ($r = 2\lambda$, $\varphi = -49.5°$) in a perspex screen. Right, pattern from the geometrically complementary disk ($r = 2\lambda$, $\varphi = +49.5°$).

influence of the magnitude of the optical thickness upon the form of the pattern can be found from the recordings along the axis of the diffracting object, c.f. Fig. 15 where the positions and heights of the extreme values in the pattern have been calculated as a function of Δ.

It is noticed that, in all the diffraction patterns, the intensity maxima and minima vary in a regular manner. Furthermore, the location of these maxima and minima is only slightly dependant on the optical path difference (See Fig. 15).

A noticeable feature in the diffraction field distribution of the phase objects, which can be seen in the recordings, is that the field outside the central region of the plane $z = 2r$ becomes nearly flat with an intensity varying about unity and that the central extremity is distorted.

Upon studying the pattern from the paraffin lens, it is remarkable how much the pattern changes from that of the corresponding "hole", considering how large a radius of curvature the paraffin lens has. Comparing Recs. 15 and 16, it is seen that there exists a conformity of the fields in the planes parallel to the aperture immediately behind the screen. The large intensity maximum in the propagation direction behind the lens, due to the converging effect of the lens-shaped phase object, is characteristic for this field. It is likewise noticeable that there are fewer rings in the diffraction pattern around the dominant maximum. From these results, it is clear that inhomogeneities in the phase object have considerable influence on the form of the diffraction field.

Institute of Optical Research, Royal Institute of Technology, Stockholm 70, Sweden.

REFERENCES

1. Andrews, C. L., Phys. Rev. *71*, 777 (1947).
2. Andrews, C. L., J. Appl. Phys. *21*, 761 (1950).
3. Severin, H., Z. Naturforschung *1*, 487 (1946).
4. Silver, S., Ehrlich, M. J., and Held, G., University of California Antenna Laboratory Report, Ser. 7, No. 185, 1952.
5. Berkefi, G. and Woonton, G. A., Eaton Electronics Research Laboratory, McGill University, Technical Report No. 24, 1952.

6. INGELSTAM, E., J. Opt. Soc. Amer. *46*, 372 (1956).
7. BRYNGDAHL, O. and INGELSTAM, E., Physica *24*, 445 (1958).
8. BOUWKAMP, C. J., Rep. Prog. Phys. *17*, 35 (1954).
9. MEIXNER, J. and ANDREJEWSKI, W., Ann. Phys. *7*, 157 (1950).
10. ANDREJEWSKI, W., Naturwissenschaften *38*, 406 (1951).
11. MEIXNER, J., Ann. Phys. *12*, 227 (1953).
12. NEUGEBAUER, H. E. J., Inst. Radio Engrs. Trans. Ant. Prop. *AP-4*, 115 (1956).
13. SEVERIN, H. and v. BAECKMANN, W., Z. ang. Phys. *3*, 22 (1951).
14. SEVERIN, H., Nuovo Cimento *9*, Suppl. No. 3, 381 (1952).
15. ANDREWS, C. L., Amer. J. Phys. *19*, 280 (1951).
16. SOMMERFELD, A., Vorlesungen über theoretische Physik, Bd. IV, Wiesbaden 1950.
17. ROSSI, B., Optics, Addison-Wesley, Reading 1957.
18. BORN, M., Optik, Springer Verlag, Berlin 1933, pp. 154–5.
19. COPSON, E. T., Proc. Roy. Soc. *A 186*, 100 (1946); *A 202*, 277 (1950).
20. MEIXNER, J., Z. Naturforschung *1*, 496 (1946); *3a*, 506 (1948).
21. NEUGEBAUER, H. E. J., J. Appl. Phys. *28*, 302 (1957).
22. SLATER, J. C., Microwave transmission, N. Y. 1942. Chap. 3.

Tryckt den 26 juni 1959

Uppsala 1959. Almqvist & Wiksells Boktryckeri AB